Some Effects of Rotation Rate on Planetary-Scale Wave Flows

Li Guoqing (李国庆)
Institute of Atmospheric Physics, Chinese Academy of Sciences, Beijing, 100080
Robin Kung
Geophysical Fluid Dynamics Institute, Florida State University, Tallahassee, Florida, U. S. A.
and *Richard L. Pfeffer*
Geophysical Fluid Dynamics Institute and Department of Meteorology, Florida State University, Tallahassee, Florida, U. S. A.
Received July 2, 1992; revised October 17, 1992

ABSTRACT

A series of experiments were performed in a rotating annulus of fluid to study effects of rotation rate on planetary-scale baroclinic wave flows. The experiments reveal that change in rotation rate of fluid container causes variation in Rossby number and Taylor number in flows and leads to change in flow patterns and in phase and amplitude of quasi-stationary waves. For instance, with increasing rotation rate, amplitude of quasi-stationary waves increases and phase shifts upstream. On the contrary, with decreasing rotation rate, amplitude of quasi-stationary waves decreases and phase shifts downstream. In the case of the earth's atmosphere, although magnitude of variation in earth's rotation rate is very small, yet it causes a very big change in zonal velocity component of wind in the atmosphere and of currents in the ocean, and therefore causes a remarkable change in Rossby number and Taylor number determining regimes in planetary-scale geophysical flows. The observation reveals that intensity and geographic location of subtropic anticyclones in both of the Northern and Southern Hemispheres change consistently with the variation in earth's rotation rate. The results of fluid experiments are consistent, qualitatively, with observed phenomena in the atmospheric circulation.

Key words: Effects of rotation, Planetary-scale wave flows, Annulus experiments

1. INTRODUCTION

Rotation is one of the basic properties in geophysical fluid dynamics. Rotation affecting a natural flow is the rotation of celestial body supporting the flow. In a reference system moving with supporting body, its rotation causes a Coriolis force $-2\rho\vec{\Omega}\times\vec{u}$ acting on relative flows, and this force gives rise to a number of specific effects. Therefore, it is very important to study effects of rotation and its time variation on baroclinic flows. It is considered, for a long time, that since variation in the earth's rotation rate is very small, its effects on the change in Rossby number determining regimes of the atmospheric circulation are so small that can be neglected. However, observations in recent years reveal that change in the axial component of atmosphere's angular momentum and change in the earth's rotation rate are closely coupled on time scales of up to several years (e. g., Dickey et al., 1985; Rosen and Salstein, 1983; Zheng et al., 1989 and references therein). These studies show that variation in earth's rotation rate is caused mainly by variation in axial component of atmosphere's angular momentum. Furthermore, some other studies reveal that the atmospheric circulation could be influenced by variation in earth's rotation rate (e. g., Teramoto, 1974; Lambeck et al., 1976; Peng et al., 1982 and Ren et al., 1986). The problem concerning the effect of

variation in earth's rotation rate on the atmospheric circulation remains unsolved and we do not know either the mechanism that the variation in earth's rotation rate affects on the atmospheric circulation.

In this paper, we present some results of laboratory experiments with a thermally driven fluid in a rotating annulus with two wave bottom topography and solely study the effects of rotation on planetary-scale wave flows. We attempt to clarify how baroclinic wave flows change if we maintain all the experimental parameters unchanged and change only a parameter of rotation rate. By comparing the experiments with observations of atmospheric circulation, we try to understand the mechanism that the variation in earth's rotation rate affects the atmospheric circulation. The paper is divided into two parts. In the first part, we briefly describe the experimental set-up and the method, and then discuss the experimental results. In the second part, we discuss the observed atmospheric phenomena related with the effects of earth's rotation change on the atmospheric circulation.

II. EXPERIMENTAL APPARATUS AND METHOD

Some gross features of general atmospheric circulation can be modelled, using a quasi-geostrophic model in which the spherical earth is replaced by the β plane. This suggests that the fundamental properties of the general atmospheric circulation are not dependent on the spherical geometry or other parameters unique to the Earth, but may be common to all rotating differentially heated fluids. Similarly to this, we can study the essential natures of atmospheric circulation, conducting rotating fluid experiments. Greenspan (1969), Hide (1983), and Chen and Li (1982) discussed the problem of similarity between the flows in rotating fluid experiments and the general atmospheric circulation. All these works confirm that laboratory simulation experiments are of important significance for testing hypotheses concerning the nature of the general circulation.

The experimental apparatus and method were described in detail by Li et al. (1986). In order to enable the reader to interpret the results of present experiments, we review briefly the main points. Fig. 1 shows a sketch of the experimental apparatus. The experimental basin B is filled with 5 centistoke silicon fluid with a depth of 10 cm measured from the middle of the

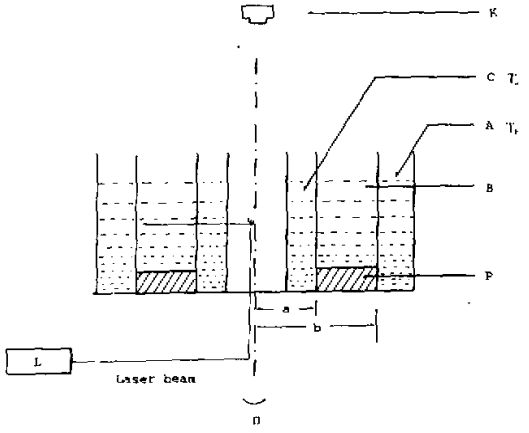

Fig. 1. Schetch of the experimental apparatus. A—warm water with temperature T_h. C—cold water with temperature T_c. B—experimental basin. K—camera. L—laser. P—topography. a = 7.5 cm, b = 15.0 cm.

topography. A constant temperature difference, $T_b - T_a = 2.0℃$, between outer and inner brass walls of the basin is maintained by circulating warm water in bath A and cold water in bath C. In order to observe the horizontal flows, we use a kind of streak photography wherein the neutrally buoyant white polyethylene particles were used as tracers. These particles were illuminated by an argon laser beam. The photographs of film sequences were digitized to put the data in numerical forms, and azimuthal (u) and radial (v) velocity components were calculated at each point of the particles. Then, we interpolated u and v to a grid of 128 azimuthal by 15 radial points. Using these data, we were able to do both Fourier and complex principal component (CPC) analyses and to evaluate many characteristic features of flow fields.

In the earlier experiments, we used a two-sinusoidal wave topography which can be described by the formula $h = H\cos 2\lambda$, where $h(\lambda)$ is the topographic height, $H = 1.75$ cm, and λ, $0 \leqslant \lambda \leqslant 2\pi$, is the azimuthal angle measured counterclockwise, from one of the ridges. The bottom surface of the annulus was latitudinally flat and the β-effect was produced only by slope of the free surface of the fluid due to rotation. The β-effect produced in this way is very small when the rotation rate is small and significant at high rotation rates. In later experiments, we used a topography with a 20° latitudinally sloped annulus bottom surface to create a constant β-effect. This is equivalent to the β-surface commonly used in numerical models. The calculation of Li et al. (1992) shows that the β-effect in experiments can be comparable to that in the earth's atmosphere.

There are two non-dimensional parameters, which determine flow regimes in the experiments, the imposed thermal Rossby number

$$R_{oT} = \frac{\alpha g D_0 (T_b - T_a)}{2\Omega^2 (b-a)^2}, \tag{1}$$

and the Taylor number

$$T_a = 4\Omega^2 (b-a)^4 / v^2 \quad , \tag{2}$$

where $\alpha = 1.05 \times 10^{-3} \mathrm{K}^{-1}$ is the coefficient of volume expansion of the fluid and g the gravitational acceleration, $D_0 = 10$cm is the mean depth of the fluid, Ω the angular velocity of the annulus rotation, $a = 7.5$ cm, $b = 15.0$ cm, and $v = 5 \times 10^{-2} \mathrm{cm}^2 \mathrm{s}^{-1}$ is kinematic viscosity of the fluid. In the present experiments, the only tested factor affecting the flow regimes is the annulus rotation rate Ω.

III. EXPERIMENTAL RESULTS

Fig. 2 illustrates the location of each of the seven analyzed experiments in $R_{oT} - T_a$ diagram. The numerical values above the diagonal indicate wavenumbers of the first principal component, and below that the wavenumbers of the second principal component of the flows. The most favourable modes are waves of wavenumber 4 for the first principal component and waves of wavenumber 2 for the second principal component.

The CPC analyzed results for six experiments with various rotation rates are shown in Fig. 3. It illustrates the contours of streamfunction along the middle circle ($R = 11.2$ cm) at the middle level ($z = 4.51$ cm) of the fluid in the time-azimuth angle plane. The modes of the first principal component are of travelling waves (a) while the dominate modes of the second principal component are of quasi-stationary waves of wavenumber 2 (b). For the first principal component waves, with increasing Ω, the phase velocity decreases while the

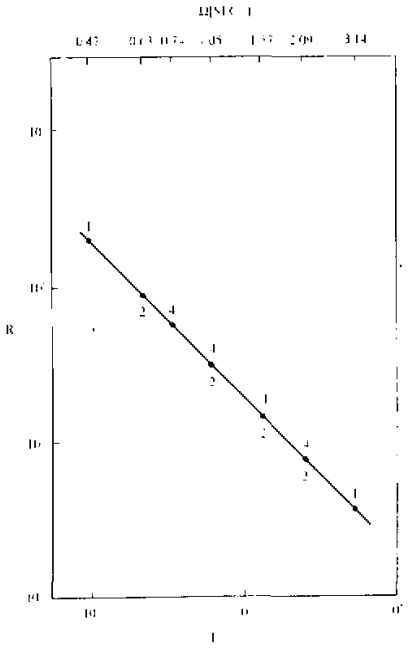

Fig. 2. Regime diagram showing location in parameter space at which the experiments were conducted. The numerical values above the diagonal with $\Delta T = 2.0$℃ designate wavenumbers of the first principals in the flows, and the numbers below the line represent wavenumbers of the second principals in the flows. *F* represents symmetric flow with very weak waves. *I* represents irregular flow.

wavenumber changes form zero at lowest rotation rate, $\Omega = 0.52\ s^{-1}$, to 4. At the largest rotation rate, $\Omega = 3.14\ s^{-1}$, the waves become irregular. For the second principal component, all the modes are of quasi-stationary waves of wavenumber 2 except that at $\Omega = 0.79\ s^{-1}$ and $\Omega = 3.14\ s^{-1}$. At $\Omega = 0.79\ s^{-1}$, a quasi-stationary wave of wavenumber 1 appears, and at the largest rotation rate, $\Omega = 3.14\ s^{-1}$, the mode turns to an irregularly travelling flow of wavenumber 4.

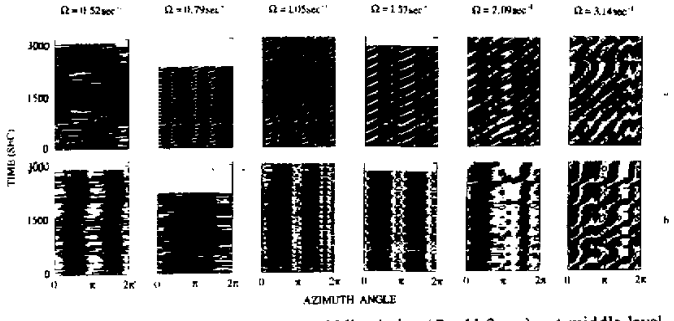

Fig. 3. Contours of streamfunction along the middle circle ($R = 11.2$ cm) at middle level ($z = 4.51$ cm) for the first (a) and second (b) principal components of the flows in time–azimuth angle plane in each of the six experiments. Contour interval is $0.1 cm^2 s^{-1}$. Negative values are shaded.

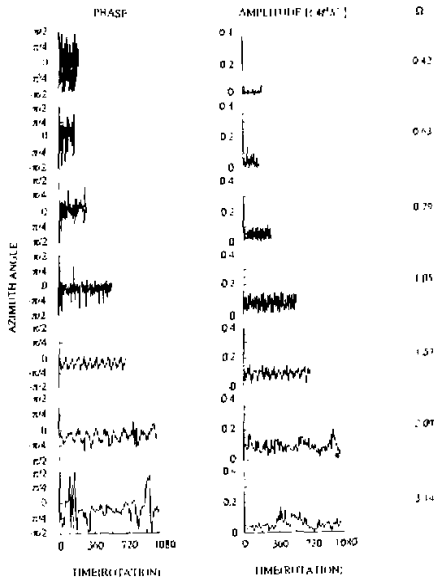

Fig. 4. Time variation in phases and amplitudes of the quasi-stationary waves in each of the experiments. The data are based on measurements taken at middle radius ($R=11.2$ cm) at middle level ($z=4.51$ cm).

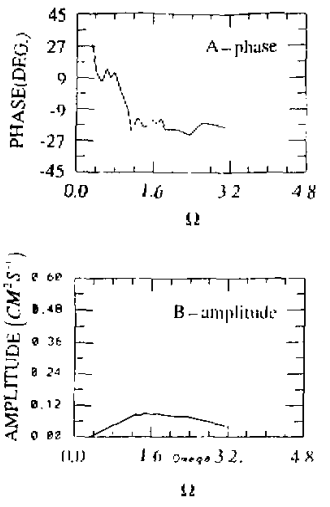

Fig. 5. Variation of time-averaged phases and amplitudes of streamfunction along the middle circle ($R=11.2$ cm) at the middle level ($z=4.51$ cm) for one of the quasi-stationary waves. The data are based on measurements in a series of twenty experiments with various rotation rate.

Fig. 4 illustrates time variation in phase angle and amplitude of the quasi-stationary waves in each of the seven experiments. The abscissa represents the time in numbers of annulus rotation. The ordinate in the left column of the figures represents azimuthal angle of the annulus, and the ordinate in the right column of the figures represents amplitude of streamfunction. The phase and amplitude vibrate upstream and downstream about its time averaged position. With increasing Ω, the range of phase vibration decreases while the range of amplitude vibration increases, and the frequency of phase and amplitude vibration decreases.

Fig.5 illustrates variation of time-averaged phases and amplitudes of streamfunction of the quasi-stationary waves along the middle circle ($R=11.2$ cm) at the middle level ($z=4.51$ cm). It is evident that, with increasing Ω, the time averaged phase location of the quasi-stationary waves shifts from $\lambda=27^\circ$ ($\Omega=0.31\ s^{-1}$) upstream to about $\lambda=-20^\circ$, and time-averaged amplitude increases at first, and then decreases after $\Omega=1.57\ s^{-1}$.

The vertical profiles of time-averaged phase of one of the stationary waves are shown in Fig. 6, using the data based on measurements taken at the fluid heights of 2.34 cm, 4.51 cm, 6.50 cm and 8.40 cm. It is evident that at smaller Ω, the phase profiles are located downstream of the topography ($\lambda>0$), and with increasing height, the profiles incline to the "west". It means that the phase angle is smaller at upper layers of the fluid than that at lower layers. With increasing Ω, the vertical profiles of phase shift upstream. Besides, the distribution shape of profiles also changes with changing Ω.

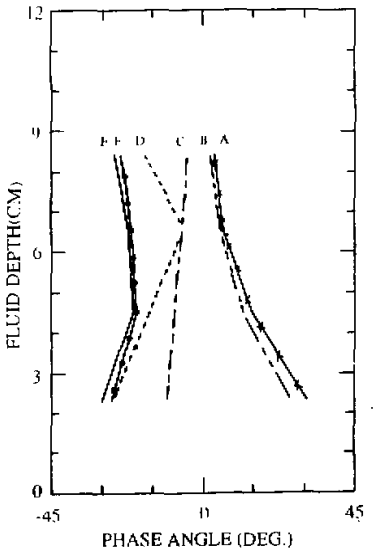

Fig. 6. Vertical profiles of time-averaged phases for one of the stationary waves in six experiments. A: $\Omega = 0.63\ s^{-1}$, B: $\Omega = 0.79\ s^{-1}$, C: $\Omega = 1.05\ s^{-1}$, D: $\Omega = 1.57\ s^{-1}$, E: $\Omega = 2.09\ s^{-1}$, F: $\Omega = 3.14\ s^{-1}$.

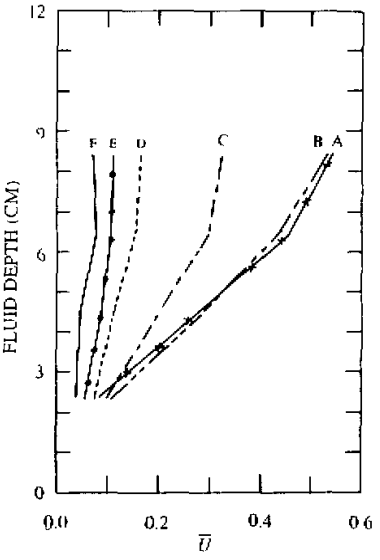

Fig. 7. Time and zonal average of the vertical profiles of $\bar{u}$ in six experiments A: $\Omega = 0.63\ s^{-1}$, B: $\Omega = 0.79\ s^{-1}$, C: $\Omega = 1.05\ s^{-1}$, D: $\Omega = 1.57\ s^{-1}$, E: $\Omega = 2.09\ s^{-1}$, F: $\Omega = 3.14\ s^{-1}$.

In addition, rotation rate affects velocity of the fluid motion. Fig. 7 illustrates the vertical profiles of time and zonally-averaged zonal velocities along the middle circle of $R = 11.2$ cm. The data used in Fig.7 are based on measurements at fluid heights of 2.34 cm, 4.51 cm, 6.50 cm and 8.40 cm in six experiments with various rotation rates. It is evident that, at lower rotation rates, the vertical profiles strongly incline with height. It means that a greater vertical gradient of zonal velocity exists in the flow with lower rotation rate. Increasing Ω reduces $\bar{u}$, and leads to a more even vertical distribution of the velocity.

All the experimental results show that the variation in rotation rate affects a lot of the flow features. Does the similar phenomenon exist in the earth's atmospheric circulation? We would study this problem in the next part of this paper.

IV. INFLUENCE OF VARIATION IN EARTH'S ROTATION RATE ON ATMOSPHERIC CIRCULATION

It is well known that the earth rotates faster in summer than it does in winter (e.g., Lambeck et al., 1980). In addition to seasonal change, the earth rotation experiences an year to year change and changes in longer time-scales. Fig. 8a illustrates seasonal variation in the long-term averaged monthly mean of the earth's rotation rate and the variation in the monthly-averaged pressure of subtropic anticyclone centres at the oceans in both the Northern and Southern Hemispheres. It shows that the pressure of subtropic anticyclone centres at the oceans in both the Northern and Southern Hemispheres increases in the summer when the earth's rotation rate is comparatively higher. Conversely, in the winter when the earth's rotation rate is lower, the pressure of the anticyclone centres decreases. Fig. 8b illustrates the seasonal variation in the long-term monthly-averaged longitude locations of the subtropic anticyclone centres at the oceans in both the Northern and Southern Hemispheres. It is evident

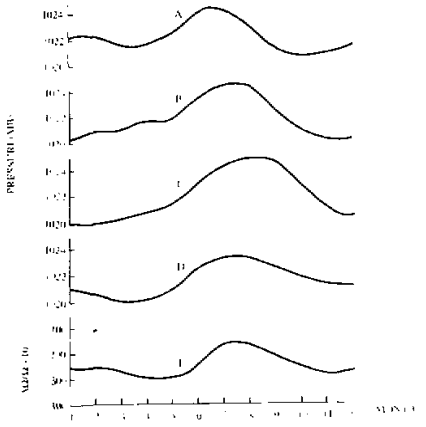

Fig. 8a. Seasonal change in monthly averaged earth's rotation rate and pressure at the centres of subtropic anticyclones at the oceans in both hemispheres. A–Indian Ocean, B–South Atlantic Ocean, C–North Atlantic Ocean, D–North Pacific Ocean, E–earth's rotation rate.

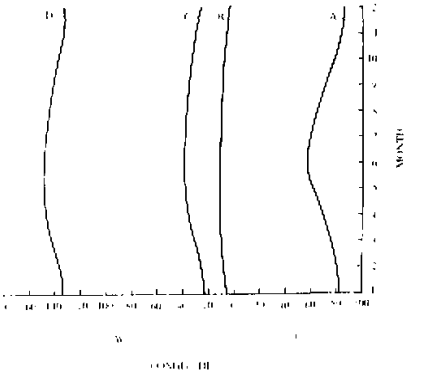

Fig. 8b. Seasonal change in longitude location of centres of subtropic anticyclones at oceans in both hemispheres. A–Indian Ocean, B–South Atlantic Ocean, C–North Atlantic Ocean, D–North Pacific Ocean.

that all the subtropic anticyclone centres at the oceans shift westward in the summer when the earth's rotation rate is comparatively higher, and return eastward back to their locations in the winter when the earth's rotation rate is lower.

The reason that the intensity and geographic location of subtropic anticyclone centres at the oceans in both hemispheres change seasonally with the same tendency is hardly explained if the seasonal variation of solar radiation is considered as the cause of change in the anticyclones because of the seasonal variations of solar radiation being opposite in both the Northern and Southern Hemispheres. The experimental results expounded in Section 3 show that increasing annulus rotation rate leads to the increase of amplitude and 'westward' shift of phase for the quasi–stationary waves (see Fig.3 and Fig.4). The seasonal variation in pressure intensity and geographic location of the subtropic anticyclones at the oceans and the variation in amplitude and phase of the quasi–stationary waves in the experimental flows due to rotation variation are very similar.

In Fig. 9 we present the curves from Peng et al. (1982) showing the long–term change in longitude and latitude locations of the subtropic anticyclone centre in North Atlantic Ocean. It is evident that the centre of the anticyclone is located southeast during the period with lower earth's rotation rate, which means that the anticyclone is more weak during this period of time. On the contrary, the centre of the anticyclone is located northwest during the period with higher earth's rotation rate, which means that the anticyclone in North Atlantic Ocean is more strong during this period of time. This kind of tendency in the variation of anticyclone location is consistent, qualitatively, with the results of fluid experiments described above (see Fig. 3, Fig. 4 and Fig. 5).

Zhao (1990) studied the consequences of decreasing the earth's rotation rate, by running the numerical GCM model of IAP. Taking one millisecond as the increment of length of day, the change to the earth's rotation rate was made instantaneously to the model initialized with

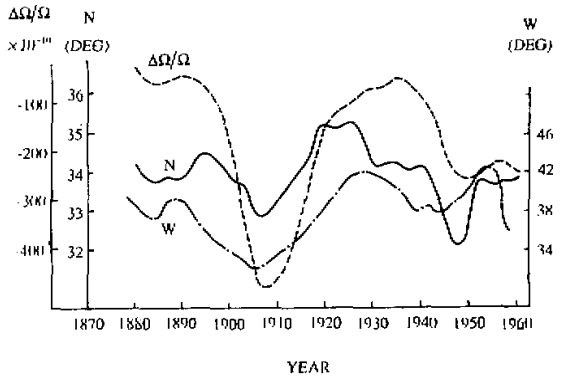

Fig. 9. 10-year running average of the subtropic anticyclone centre locations in North Atlantic Ocean and earth's rotation rate, $\Delta\Omega/\Omega$ (after Peng et al.). N-latitude, W-longitude.

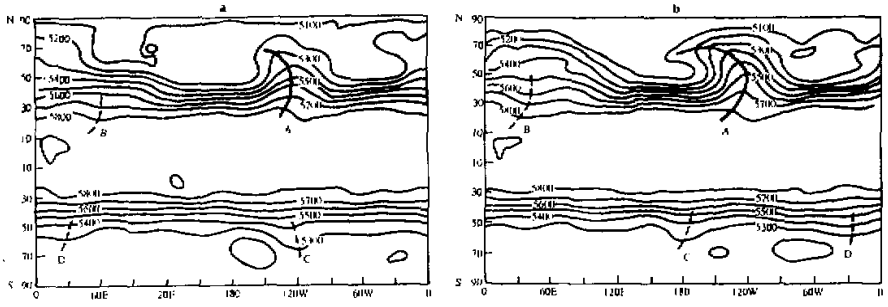

Fig. 10. 500 hPa height charts(m) showing the response of atmospheric circulation to decreasing earth's rotation rate (from Zhao, 1990). (a) chart integrated for one month from Dec. 1, 1988 with increasing length of day of 1 millisecond, (b) chart integrated for one month from Dec. 1, 1988 without changing length of day.

the observed meteorological fields of December first, 1988. He integrated the model for two cases, one with and one without decreasing the earth's rotation rate. The 500 hPa height contours after integration for one month are shown in Fig.10a for the case with decreasing the earth's rotation rate and in Fig. 10b for the control case without changing the earth's rotation rate. It is evident that the troughs and the ridges in both hemispheres are comparatively weak and are located east when the earth's rotation rate is low (Fig.10a). On the contrary, it seems that all the troughs and ridges in both hemispheres are enhanced and located comparatively west when the earth's rotation rate is high (see Fig.10b). It seems that the numerical modelling results also coincide with the fluid experiments described above.

V. MECHANISM OF INFLUENCE OF EARTH'S ROTATION RATE ON ATMOSPHERIC CIRCULATION

In the introduction of this paper, we have mentioned that the magnitude of variation in earth's rotation rate is very small and causes a negligible change in Rossby number. Then, how does the change in earth's rotation rate influence the atmospheric circulation? Considering the earth's crust, ocean and atmosphere as a system of conservation of angular momentum, namely,

$$J = J_e + J_a + J_0 = \text{const}, \tag{3}$$

where J is angular momentum of the system, and the subscripts e, a and o represent the earth's crust, atmosphere and ocean, respectively, and letting I represent the moment of inertia, and Ω the angular velocity, we may rewrite (3) as follows,

$$J = I_e\Omega_e + I_a\Omega_a + I_o\Omega_0 = \text{const} \ . \tag{4}$$

Differentiating (4), we obtain

$$\Delta J = \Omega_e \Delta I_e + I_e \Delta\Omega_e + \Omega_a \Delta I_a + I_a \Delta\Omega_a + \Omega_o \Delta I_o + I_o \Delta\Omega_o = 0.$$

It can be proved that $\Omega_e \Delta I_e$, $\Omega_a \Delta I_a$, and $\Omega_o \Delta I_o$ are of second-order small terms to be neglected, and we have

$$\Delta\Omega_e = -\frac{I_0}{I_e}\Delta\Omega_o - \frac{I_a}{I_e}\Delta\Omega_a \ . \tag{5}$$

In conformity with Allen (1973), $I_e = 8.04 \times 10^{44}\,\text{g.cm}^2$, $I_a = 1.41 \times 10^{39}\,\text{g cm}^2$, and $I_o = 2.94 \times 10^{41}\,\text{g cm}^2$, we obtain

$$\Delta\Omega_e = -3.658 \times 10^{-4}\Delta\Omega_o - 1.757 \times 10^{-6}\Delta\Omega_a \ . \tag{6}$$

Expression (6) implies that $\Delta\Omega_e$, the change in earth's rotation rate, causes a change in zonal velocity of ocean current $\Delta\Omega_o$, which is 10^4 times large as $\Delta\Omega_e$, and a change in zonal velocity of wind in the atmosphere, $\Delta\Omega_a$, which is 10^6 times as large as $\Delta\Omega_e$, and the direction of $\Delta\Omega_e$ is opposite to that of $\Delta\Omega_a$ and $\Delta\Omega_o$.

For monthly average, taking $\Delta\Omega_e / \Omega = 40 \times 10^{-10}$, we obtain $\Delta\Omega_a = -0.166 \times 10^{-6}$s, and $\Delta\Omega_o = 0.795 \times 10^{-9}$s. Since $\Delta u = R\Delta\Omega$ and $\Delta u_\varphi = \Delta u \cdot \cos\varphi$, where φ denotes latitude and R the mean radius of the earth, we can calculate the change in zonal components of wind velocity in the atmosphere and of ocean currents, which are caused by the change in the earth's rotation rate. The calculated results are listed in Table 1. It shows

Table 1. Change in Zonal Velocity of Wind in the Atmosphere and of Ocean Currents due to the Change in Earth's Rotation Rate of $\Delta\Omega_e / \Omega = 40 \times 10^{-10}$

Latitude (deg)	Δu_a (m s^{-1})	Δu_o (cm s^{-1})
0	1.05	0.51
10	1.04	0.50
20	0.99	0.48
30	0.91	0.44
40	0.81	0.39
50	0.68	0.33
60	0.50	0.25
70	0.36	0.17
80	0.18	0.09
90	0.00	0.00

that the change in the earth's rotation rate causes quite a large variation in zonal velocity of wind in the atmosphere and of ocean currents. It is not difficult to imagine that this is bound to lead to quite a large change in Rossby number, which determines regimes in geophysical

flows. For instance, taking $u = 10\text{m s}^{-1}$ as the velocity of west wind in the troposphere, the change in the earth's rotation rate causes a Δu of about one tenth of u. Therefore, the Rossby number also changes about one tenth of its magnitude. The experimental results described in the first part of the paper show that the regime of large-scale baroclinic flows is bound to respond to such a large change in Rossby number.

VI. CONCLUSIONS

The fluid experiments show that regimes of planetary-scale baroclinic flows are determined by Rossby number and Taylor number in the flows. The change in rotation rate of the fluid system causes variation in Rossby number and Taylor number and leads to change in flow regimes. For instance, increasing rotation rate causes an amplitude increase and phase decrease of quasi-stationary waves. On the contrary, decreasing rotation rate leads to amplitude decrease and phase increase of quasi-stationary waves. Phenomena similar to the experimental results exist in the earth's atmospheric circulation. The magnitude of change in earth's rotation rate is very small, and rotation rate change itself causes a negligible change in Rossby number. However, the change in earth's rotation rate can make enormous change in zonal components of wind in the atmosphere and of ocean currents. Therefore, it causes quite a large change in Rossby number in the geophysical flows and leads to change in atmospheric circulation. During the period with increased earth's rotation rate, all the subtropic anticyclones at oceans in both hemispheres intensify and their geographic locations are to the west. On the contrary, during the period with decreased earth's rotation rate, all the anticyclones weaken and their geographic locations are to the east.

The authors are grateful to Mr. R. Arbogast and W. Auld for bulk of the analysis and graph programming, Mr. G. Arnord for assistance in doing the laboratory experiments and Mr. C. Lewis for his professional supervision of the digitizing personnel and data scrutiny and correction of errors. This research was supported in part by NSF Grant No. ATM-9012093 and in part by ONR Contract No. N00014-91-J-1825.

REFERENCES

Allen, C. W. (1973), Astrophysical quantities, 3rd. ed., London Athlone.

Chen, R. R. and Li Guoqing (1982), An experimental simulation on the mechanical effect of Tibetan Plateau on zonal circulation of stratified atmosphere, *Sci. Sin. Ser. B*, **25**: 1091-1102.

Dickey, J. O., T. M. Eubanks and J. A. Steppe (1985), High accuracy earth rotation and atmospheric angular momentum, In: Nato advanced research workshop on earth rotation: solved and unsolved problems.

Greenspan, H. P. (1969), *The theory of rotating fluids*, Cambridge Univ. Press, London.

Hide, R. (1983), On the dynamics of rotating fluids and planetary atmospheres: a summary of some recent work, *Pure and Applied Geophysics*, Basel, **121(3)**: 365-374.

Lambeck, K. and A. Cazenave (1976), Long term variations in the length of day and climatic change, *Geophys. J. Roy. Astron. Soc.*, **46**: 555-573.

——(1980), *The earth's variable rotation: Geophysical causes and consequences*, Cambridge, Cambridge Univ. Press.

Li, G. Q., R. Kung and R. L. Pfeffer (1986), An experimental study of baroclinic flows with and without two-wave bottom topography, *J. Atmos. Sci.*, **43**: 2585-2599.

Li Guoqing, R. Kung and R. L. Pfeffer (1992), A fluid experiment of large-scale topography effect on baroclinic wave flows, *Advances in Atmos. Sci.*, **9**: 17-28.

Peng Gongbing, Lu Wei and Yin Yanzhen (1982), Response of climate and its atmospheric circulation factors on change in the earth's rotation rate, *Acta Meteor. Sin.*, **40**: 209-218.

Pfeffer, R. L., R. Kung and G. Q. Li (1989), Topographically-forced waves in a thermally driven rotating annulus

of fluid-experiment and linear theory. *J. Atmos. Sci.*, **46:** 2331–2343.

Pfeffer, R. L., J. Ahlquist, R. Kung, G. Q. Li and Y. Chang (1990), A study of baroclinic wave behavior over bottom topography using complex principal component analysis of experimental data. *J. Atmos. Sci.*, **47:** 67–81.

Ren Zhenqiu and Zhang Suqin (1986), Deceleration of earth's rotation and formation of El Nino, *Acta Meteor. Sin.*, **44:** 411–416.

Rosen, R. D. and D. A. Salstein (1983), Variations in atmospheric angular momentum on global and regional scales and length of day, *J. Geophys. Res.*, **88:** C9, 5451–5470.

Teramoto, T. (1974), Large-scale variation of air-sea system in the North Pacific Ocean, *Science (Japan)*, **44:** 685–693.

Zhao Wenje (1990), Numerical experiment on the effect of deceleration of earth rotation on the atmosphere., Graduation thesis. Institute of Atmospheric Physics, Chinese Academy of Sciences.

Zheng Dawei, Luo Shifang and Song Guoxuan (1989), Interannual variation of earth rotation, El Nino events and angular momentum, *Science in China, Ser. B.* **32(6):** 729–736.